Lamellar morphology induced by two-step surface-directed spinodal decomposition in binary polymer mixture films

ARTICLE *in* THE JOURNAL OF CHEMICAL PHYSICS · FEBRUARY 2008

Impact Factor: 2.95 · DOI: 10.1063/1.2819676 · Source: PubMed

2 AUTHORS, INCLUDING:

Xu-Ming Xie
Tsinghua University
168 PUBLICATIONS **1,590** CITATIONS

SEE PROFILE

Lamellar morphology induced by two-step surface-directed spinodal decomposition in binary polymer mixture films

Li-Tang Yan and Xu-Ming Xie[a)]
Advanced Materials Laboratory, Department of Chemical Engineering, Tsinghua University, Beijing 100084, People's Republic of China

(Received 31 August 2007; accepted 7 November 2007; published online 15 January 2008)

A novel process for obtaining ordered morphology on the basis of two-step surface-directed spinodal decomposition is numerically investigated. The formation mechanism and evolution dynamics of this process are also discussed in detail. The calculated results of the chemical potential demonstrate that the equilibration state at the first quench affects the competition between the surface potential and the chemical potential in the bulk, leading to a surprising lamellar structure at the second further quench. It is also found that the lamella formation obeys the logarithmic growth. These results could provide a new approach for fabricating ordered structure of polymer materials and stimulate experimental studies based on this subject. © *2008 American Institute of Physics*. [DOI: 10.1063/1.2819676]

I. INTRODUCTION

Phase separation in binary mixtures commonly leads to complex patterns of domains after a temperature quenching into an unstable state.[1] The morphology of such systems could be either interconnected domain structures or isolated clusters, depending mainly on the relative concentrations of the two phases. On the other hand, the opportunity to create new useful materials continues to motivate considerable research on the ordered phase morphology. It is always difficult to experimentally obtain a well-defined lamellar pattern in which the layers are mostly parallel to each other just like block copolymers, due to the difficulty for eliminating the structure defects in spatially period pattern. Externally applied perturbations can, however, direct the separation process to create ordered phase domain structure. The possible control over the domain curvature and orientation includes shear flow,[2] confinements,[3] patterned surface,[4] temperature inhomogeneity,[5] and the presence of period oscillatory particles with a preferential additive to one of the immiscible phases.[6] Hence, researchers can tailor domain patterns of polymer materials and obtain new ordered structures through tuning these factors.

A more controlled approach to phase separation in polymer blends was first explored by studying surface-directed spinodal decomposition (SDSD).[7] In this case, the surface or interface is completely or partially wetted by the preferential component and becomes the origin of anisotropic spinodal decomposition waves which propagate into the bulk perpendicular to the surface.[8] By varying the concentration of the composition or quench depth, the growth of the wetting layer can exhibit different mechanisms, including diffusion limited growth law, logarithmic growth law, and Lifshitz-Slyozov (LS) growth law.[9] The nature of the phenomena is due to the interaction between the surface potential and the chemical potential in the bulk.[9] Generally speaking, although the surface potential can induce greater amplitude anisotropic fluctuation of the concentration, the phase morphology in the bulk still presents typical interconnected domain structures or isolated clusters when a SDSD system is quenched directly from one-phase region to the two-phase region of its phase diagram because the chemical potential in the bulk has stronger effects on it.[8–10] Moreover, as the two-step phase separation without surface has been fully explored experimentally and numerically,[11] there are almost no data on how the phase morphology forms during two-step quench process of SDSD which may lead to novel phase morphologies.

In this paper, we report a simple and controllable strategy to produce ordered phase morphology. The novel method is on the basis of two-step quench process of SDSD with two surfaces at the top and bottom sides. First, the polymeric mixture is quenched to an equilibrium state where the quench depth is only a little deeper than the critical point. During this equilibration, phase separation does not occur in the bulk and only a layer of the preferential component for the surface forms along the surface by wetting. The system is allowed to evolve until an approximate stable state is achieved. Then, the system is quenched into the two-phase region. Stripes parallel to the surface, termed as lamellar morphology, can be obtained.

II. MODEL AND NUMERICAL PROCEDURE

The dynamics of this process is modeled by coupling Flory–Huggins–de Gennes (FHdG) equation[12] with Cahn-Hilliard-Cook (CHC) equation.[13] The detailed deduction of the model has been given in our previous work.[14] In order to keep the integrity of this paper, we briefly review it here.

For simplicity, a symmetric mixtures of two polymer species, A and B, with chain lengths $N_A=N_B=N$ is considered. Hydrodynamic effects, which may play an important role in the very late stage of phase separation, are neglected

[a)]Author to whom correspondence should be addressed. Electronic mail: xxm-dce@mail.tsinghua.edu.cn.

throughout as we only consider a large molecular weight system where the hydrodynamic interactions can be neglected.[15] CHC equation can be written as

$$\frac{\partial \phi}{\partial t} = M\nabla^2 \frac{\delta F\{\phi(r,t)\}}{\delta \phi(r,t)} + \eta(r,t), \tag{1}$$

where $\phi(r,t)$ is the local fraction of component at point r and time t. $\eta(r,t)$ is thermal noise. M is the mobility, assumed to be constant. In order to study phase separation in polymer mixture, for F, the FHdG free energy (in units of k_BT) is chosen and is given by

$$F(\phi) = \int_V dr \left[\frac{\phi}{N} \ln(\phi) + \frac{(1-\phi)}{N} \ln(1-\phi) + \chi\phi(1-\phi) + \frac{b^2}{36\phi(1-\phi)} |\nabla\phi|^2 \right], \tag{2}$$

where χ is the temperature-dependent Flory-Huggins dimensionless interaction parameter and b is the Kuhn statistical segment length.[12] The integral is performed over the volume V of the sample. In terms of the deduction of Puri and Binder,[16] the boundary conditions of SDSD dynamic model based on CHC equation can be described by two partial differential equations. The first equation is defined as

$$\frac{\partial \phi(x,z_0,\tau)}{\partial \tau} = -h_1 - g\phi(x,z_0,\tau) + \gamma \left. \frac{\partial \phi(x,z,\tau)}{\partial z} \right|_{z=z_0}, \tag{3}$$

where h_1, g, and γ are three parameters characterizing the static surface diagram.[16] z_0 is the location of the surface. It has been proven that the calculated results are more precise if Eq. (3) is coupled into the dynamic model.[14] Thus, by lumping together Eqs. (1)–(3) and by rescaling into a dimensionless form, the dynamic equation can be obtained as follows:

$$\frac{\partial \phi(r,\tau)}{\partial \tau} = \frac{1}{2}\nabla^2 \left[\frac{\chi_c}{2(\chi_f - \chi_s)} \ln \frac{\phi}{1-\phi} - \frac{2\chi}{\chi_f - \chi_s}\phi + \frac{2\phi - 1}{36\phi^2(1-\phi)^2}(\nabla\phi)^2 - \frac{1}{18\phi(1-\phi)}\nabla^2\phi + \left(-h_1 - g\phi + \gamma \left. \frac{\partial \phi}{\partial z} \right|_{z=0} \right) \delta(z) \right]. \tag{4}$$

$\chi_c = \chi_s$ is the spinodal value of χ at $\phi = \phi_0$, i.e., $\chi_s = 1/[2N\phi_0(1-\phi_0)]$, where ϕ_0 is the initial average concentration of component A, with $\phi_0 = 0.5$ for the critical condition in the present simulation. χ_f is the deepest quench. $\bar{r}$ and τ are rescaled spatial and temporal variables, respectively, given by $\bar{r} = (|\chi_f - \chi_s|)^{1/2} r/l$ and $\tau = NM(\chi_f - \chi_s)^2 t/l^2$. $\delta(x)$ is the Dirac-delta function, ensuring that the surface free energy only affects $z_0 = 0$ and $L+1$, where L is the maximum value of z. A second boundary condition, $\Delta J|_{z=z_0} = 0$, where J, defined as $J = \nabla \delta F/\delta\phi$, is the polymer flux and is used to ensure that the flux of polymer components through the surface boundary is zero, which enforces conservation of the order parameter.[16] The noise term has been neglected because we only consider a system without noise or with small amplitude noise. However, a small random fluctuation in volume fraction, with the magnitude of $\pm 1 \times 10^{-3}$, is added to each lattice at the start of a simulation for the occurrence of phase separation.[17]

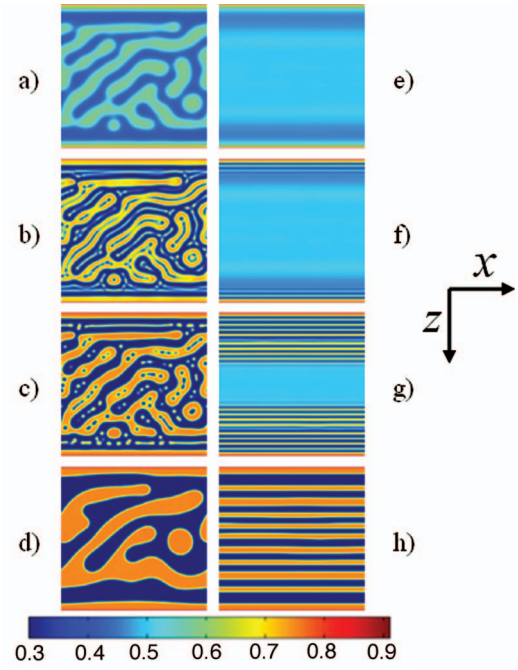

FIG. 1. (Color) Comparison of morphology evolution following two-step SDSD with the same second quench depth, $\varepsilon_2 = 0.1$. The first quench depth of the left-hand side is $\varepsilon_1 = 0.01$, compared to $\varepsilon_1 = 0.001$ of the right-hand side. The color bar indicates the concentration of the preferentially wetting component for the surface. The second quench times correspond to τ_2 = [(a) and (e)] 0, [(b) and (f)] 40, [(c) and (g)] 100, and [(d) and (h)] 10 000.

Equation (4) was numerically resolved by the finite difference method[17] on a 300×300 lattice. Periodic boundary conditions were applied in the parallel direction. $h_1 = -1.5$, $g = 0.1$, $\gamma = 0.1$, and $N = 200$ were set in all simulations. To simplify the numerical procedure and to avoid having to rescale the lattice, $\chi_f - \chi_s$ was chosen to be the same before and after the quench and was fixed at 0.0133 throughout simulations. The Δt (time step) value used during the temporal discretization was 1×10^{-4}, and the spatial discretization step was $\Delta\bar{r} = 0.5$.

III. RESULTS AND DISCUSSIONS

A dimensionless parameter, ε, which is defined as $\varepsilon = (\chi - \chi_c)/\chi_c$, denotes the quench depth in this work. ε_1 and ε_2 indicate the first and second quench depths, respectively. The first quench time τ_1 was set to 10 000 for all simulations. A comparison of the development of the morphology following a second quench depth is shown in Fig. 1: one of the polymer blends has undergone phase separation at the first quench [Fig. 1(a), $\varepsilon_1 = 0.01$] and the other has undergone equilibration at the first quench [Fig. 1(e), $\varepsilon_1 = 0.001$]. Both these two cases have the same value of the second quench depth, i.e., $\varepsilon_2 = 0.1$. In Figs. 1(a)–1(d), clearly, when a second quench is applied to a point further inside the unstable region, smaller secondary domains appear briefly in the primary domains obtained from the first quench depth. It is the typical morphology of two-step phase separation.[11] Eventually, the original morphology is returned but with higher concentration contrast between two components [Fig. 1(d)].

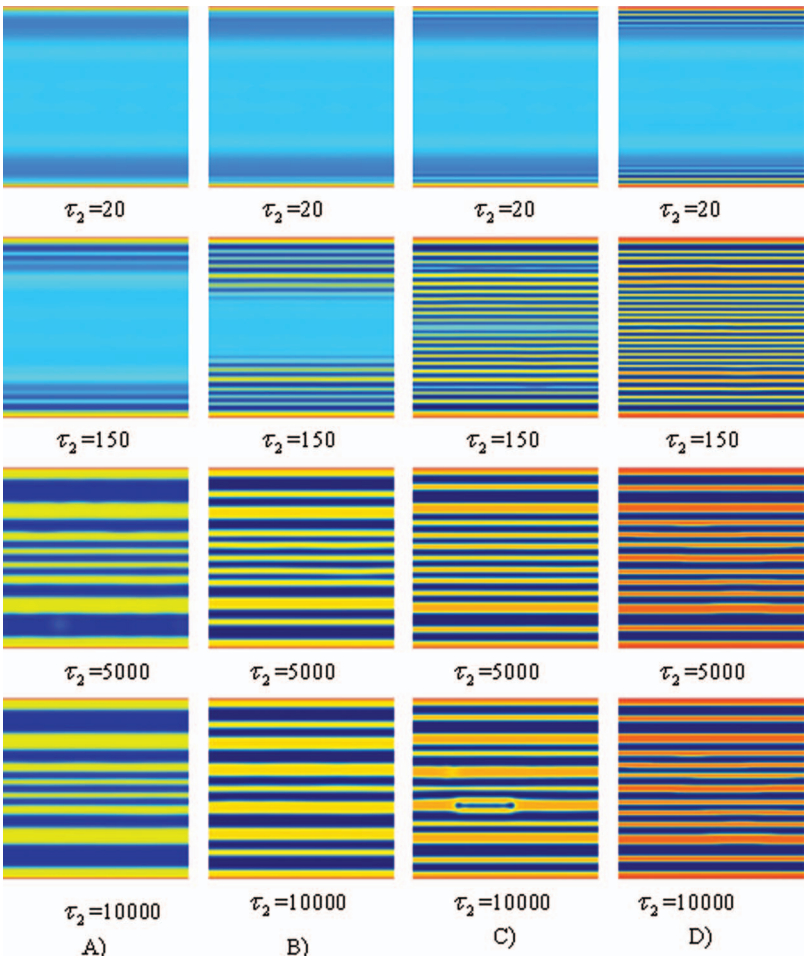

FIG. 2. (Color) Development of the polymer morphology following different second quench depths with $\varepsilon_1=0.001$, (a) $\varepsilon_2=0.04$, (b) 0.06, (c) 0.08, and (d) 0.12.

However, when the blends are quenched from an equilibration [Fig. 1(e)] to an unstable state in the two-phase region, instead of the typical two-step phase separation morphology as Figs. 1(a)–1(d), the lamellar structure appears near the wetting layer at the initial stage [Fig. 1(f)]. Then, it propagates into the bulk and coarsens to larger scale lamellar structure gradually [Figs. 1(g) and 1(h)].

The similar ordered structures can be found in different second quench depths, which have been listed in Fig. 2. It can be seen that the lamellar structure occurs near the wetting layer and penetrates into the bulk gradually when different deeper quench depths have been added. Then, the order structure can coarsen into large-size case with the increasing time. Moreover, one can found that a deeper second quench depth corresponds to an earlier appearance of the lamellar structure near the wetting layer.

Figure 3 shows the averaged profiles in the z direction at different times. The averaged profiles are obtained by averaging the concentration profile $\phi(x,z,\tau)$ of the parallel cross sections along the z axis as Eq. (5) with $N_x=\phi_{\mathrm{av}}(x,0,\tau)$ for a single run and then ensemble averaging over ten different runs,

$$\phi_{\mathrm{av}}(z,\tau)=\frac{1}{N_x}\sum_x \phi(x,z,\tau). \tag{5}$$

It can be observed from this figure that the great composition fluctuation preferentially occurs near the wetting layer once the second deep quench is added. It should be noted that there is no any phase separation in the bulk. Then, the second quench induces phase separation exactly following the one-dimensional composition fluctuation and the fluctuation wave penetrates into the bulk gradually. In the final stage, the fluctuation wave expands to the whole system and the lamellar structure forms.

For the sake of understanding the role of the equilibration in the formation of the lamellar structure, the chemical potential $\mu_t(x,z)$, which can be calculated from the terms in the parentheses of Laplacian in Eq. (4), is considered. The fluctuation degree of the chemical potential can be used to characterize the activity of the blends, and a stronger fluctuation of the chemical potential indicates a higher possibility for the occurrence of phase separation.[1] For convenience in comparing the fluctuation degree of the chemical potential, the value of $\mu_t(x,z)$ in each lattice is reduced by that of $\mu_t(1,1)$, leading to the relative chemical potential $\mu(x,z)$. Figures 4(a)–4(c) illustrate the evolution of $\mu(x,z)$ during equilibration ($\varepsilon=0.001$), where the effects of surfaces are not included in it. It can be seen that the fluctuation of the chemical potential becomes smaller with the increasing time, demonstrating that the activity of the blends becomes weak and phase separation is more difficult to occur. Thus, the equilibration at the first quench really inhibits the phase separation in the bulk. Then, the anisotropic waves induced by the surface have enough time to propagate into the bulk easily and

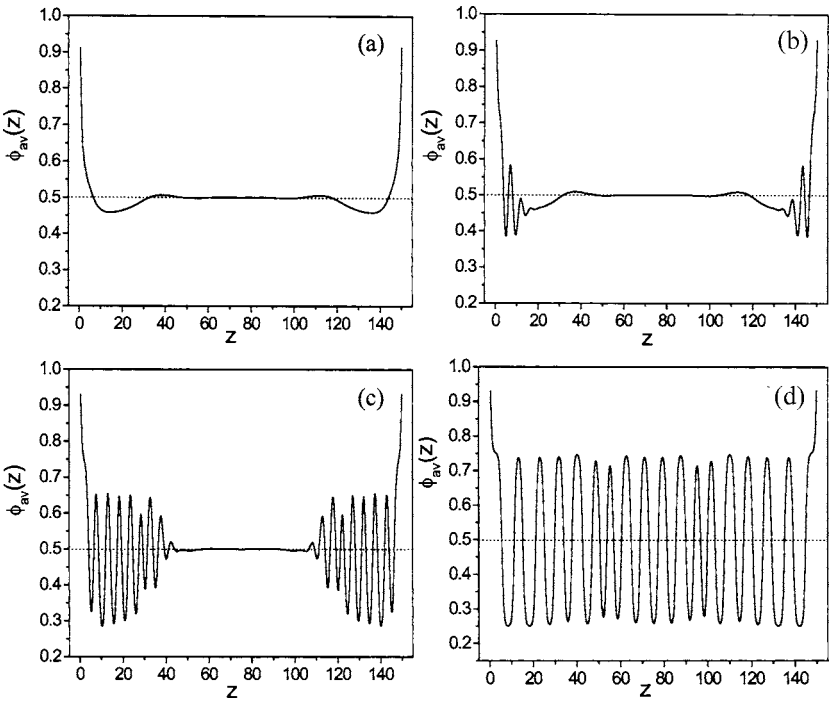

FIG. 3. Plots of laterally averaged profile $\phi_{av}(z)$ against z for different times where $\varepsilon_1=0.001$ and $\varepsilon_2=0.1$. (a) $\tau_2=0$, (b) 40, (c) 100, and (d) 500.

dominate the phase morphology in the second quench, leading to the lamellar structure. However, when phase separation has occurred in the first quench, the fluctuation degree of the chemical potential is very strong [Fig. 4(d)], and the bulk undergoes typical two-step phase separation in the second quench [Figs. 1(e)–1(h)]. One should note that the formation mechanism of the lamellar structure is basically different from that of the general confined phase separation which is purely induced by the spatial limitation inside cylindrical pores or between two substrates.[10] As a matter of fact, the large scale ordered structure cannot almost be obtained through the general confined phase separation. It should be pointed out that the formation of the lamellar structure has a tight relation with the composition noise which can affect the occurrence of the spinodal decomposition in the bulk. Clearly, as the lamellar states are lone lived, they are transient and not metastable. Thus, limited conditions can be selected for the experimental observations.

Next, we consider the evolution dynamics of the lamellar structure. Figure 5 displays a series of snapshots to demonstrate a detailed process of the lamellar growth following two-step SDSD with $\varepsilon_1=0.001$ and $\varepsilon_2=0.1$. One can find that a neck zone forms in the thin lamella between two wide lamellas. Then, the thin lamella shrinks and becomes shorter and shorter, accompanying with the growth of two thick lamellas. Eventually, the thin lamella disappears. In order to examine the evolution dynamics mechanism of the lamellar structure quantitatively, the average lamellar thickness L_a is defined and calculated. To calculate L_a, the laterally averaged profile $\phi_{av}(z)$ against z is obtained first. Figure 6(a) is an

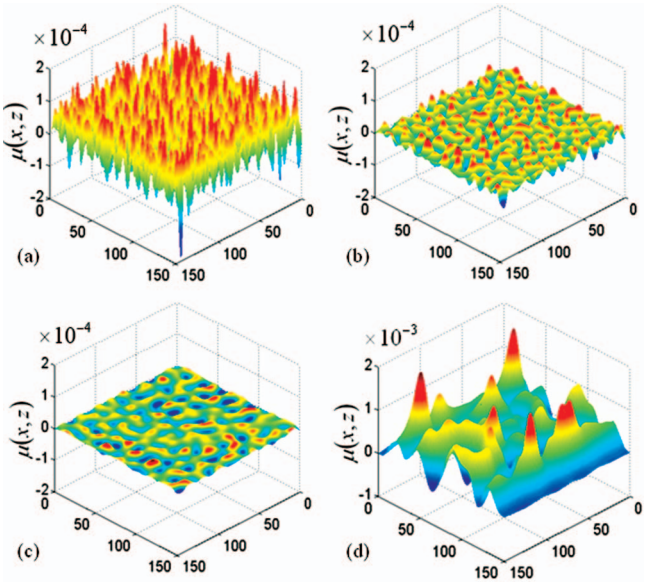

FIG. 4. (Color) Three-dimensional diagrams showing the chemical potential $\mu(x,z)$ for a critical quench with $\varepsilon=0.001$ at different times, (a) $\tau=20$, (b) 100, and (c) 500. The chemical potential corresponding to Fig. 1(a) is shown in (d).

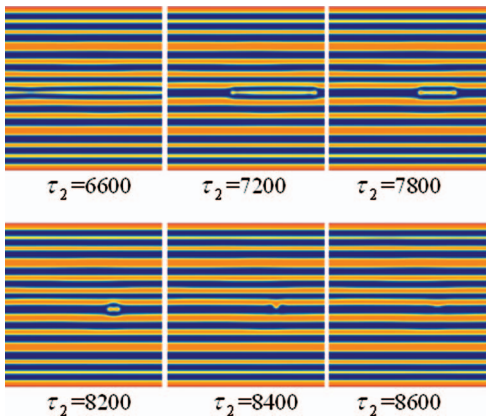

FIG. 5. (Color) The dynamic process of lamellar growth following two-step SDSD with $\varepsilon_1=0.001$ and $\varepsilon_2=0.1$. The color bar and the coordination are the same as those in Fig. 1.

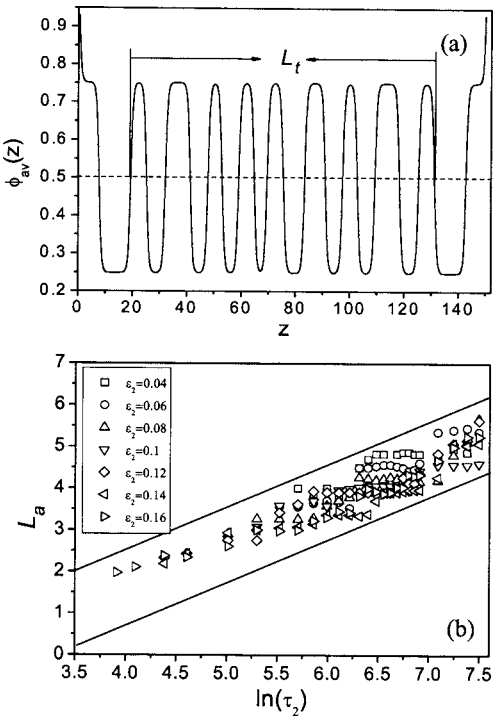

FIG. 6. (a) Plot of laterally averaged profile $\phi_{av}(z)$ against z for the pattern depicted in Fig. 1(h). (b) Plots of average lamellar thickness L_a against logarithmic second quench time $\ln(\tau_2)$ with $\varepsilon_1=0.001$. The slopes of both two lines in this figure are 1.

example showing the laterally averaged profile of Fig. 1(h). A periodicity and high degree of concentration fluctuation correspond to the lamellar structure, compared to the random fluctuation in general SDSD.[9] As shown in Fig. 6(a), the total lamellar thickness L_t can be measured from the z position with the value of 0.5 in the right side of the first peak to that in the left side of the last peak. The total number of peaks is marked with N_t. Then, the average lamellar thickness L_a is defined as $L_a=L_t/N_t$. The temporal evolution of L_a with different second quench depths is shown in Fig. 6(b) in a logarithmic time scale. The lines in the figure indicate that the growth of the average lamellar thickness obeys the logarithmic growth law, i.e., $L_a \propto \ln(\tau)$.

This dynamics mechanism can be understood as follows. Let l_0 be the character length and increases by coarsening as ${l_0}^{\alpha} \propto \tau$. In the case of general phase separation system, $\alpha=3$, which is known as the LS law.[18] In the present case, however, the domains are lamellas. It can be found from Fig. 7 that the domain size in the direction parallel to the lamella is approximately unchangeable and the growth of the lamellar structure only occurs in the direction perpendicular to the lamella. Basically, the situation is similar to the case of one-dimensional kink dynamics of a conserved order parameter system.[19] Thus, LS law cannot be applied, but l_0 obeys a logarithmic growth, that is, $\alpha=\infty$. One should note that this mechanism is obtained on the basis of the system without the effect of noise and in two-dimensional space. However, noise may affect the dynamical process and the case in three-dimensional space may be different, which will be discussed in detail in our next works.

In summary, we have first demonstrated that a lamellar morphology can be obtained when the SDSD system is quenched to an equilibration state and then be applied to a point further inside the two-phase region of the phase diagram.[20] The equilibration state changes the interplay between the surface potential and the chemical potential in the bulk. Thus, the anisotropic waves, induced by the surface, dominate the phase morphology in the second quench, leading to the lamellar structure. The simulated results also indicate that the lamella grows with the logarithmic law. This novel approach may lead to develop regular morphology with unusual physical properties and has important technical application. We hope that our results will stimulate experimental work on this subject.

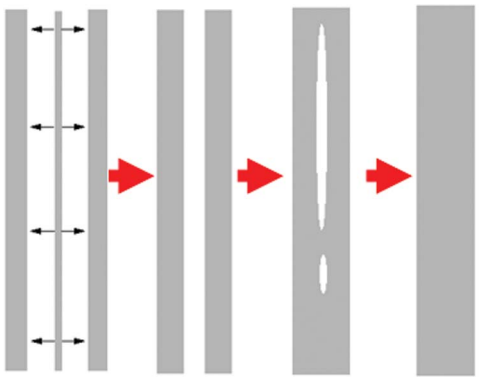

FIG. 7. (Color online) The schematic diagram illustrating the dynamics mechanism of the lamellar structure.

ACKNOWLEDGMENTS

Financial support from the National Natural Science Foundation of China (Nos. 50573088, 20174022, and 10334020) is highly appreciated.

[1] H. Furukawa, Adv. Phys. **37**, 703 (1985); A. J. Bray, *ibid.* **43**, 357 (1994).
[2] Z. R. Chen, J. A. Kornfield, S. D. Smith, J. T. Grothaus, and M. M. Satkowski, Science **277**, 1248 (1997).
[3] S. Zhu, Y. Liu, M. H. Rafailovich, J. Sokolov, D. Gersappe, D. A. Winesett, and H. Ade, Nature (London) **400**, 49 (1999).
[4] M. Böltau, S. Walheim, J. Mlynek, G. Krausch, and U. Steiner, Nature (London) **391**, 877 (1998).
[5] T. Hahimoto, J. Bodycomb, Y. Funaki, and K. Kimishima, Macromolecules **32**, 952 (1999).
[6] H. Tanaka, A. J. Lovinger, and D. D. Davis, Phys. Rev. Lett. **72**, 2581 (1994).
[7] R. A. L. Jones, L. Norton, E. J. Kramer, F. S. Bates, and P. Wiltzius, Phys. Rev. Lett. **66**, 1326 (1991).
[8] S. Puri, J. Phys.: Condens. Matter **17**, R101 (2005); S. Puri and K. Binder, Phys. Rev. A **46**, R4487 (1992); Phys. Rev. E **56**, 6991 (1997).
[9] S. Puri and K. Binder, Phys. Rev. Lett. **86**, 1797 (2001); Phys. Rev. E **66**, 061602 (2002).
[10] A. J. Liu, D. J. Durian, E. Herbolzheimer, and S. A. Safran, Phys. Rev. Lett. **65**, 1897 (1990); S. K. Das, S. Puri, J. Horbach, and K. Binder, Phys. Rev. E **72**, 061603 (2005).
[11] M. Okada, K. D. Kwak, and T. Nose, Polym. J. (Tokyo, Jpn.) **24**, 215 (1992); H. Tanaka, Phys. Rev. E **47**, 2946 (1993); T. Hashimoto, H. Masaki, and H. Jinnai, J. Chem. Phys. **112**, 6886 (2000); I. C. Henderson and N. Clarke, Macromolecules **37**, 1952 (2004); M. Fialkowski and R. Holyst, J. Chem. Phys. **117**, 1886 (2002).
[12] P. J. Flory, *Principles of Polymer Chemistry* (Cornell University Press, Ithaca, NY, 1953); P. G. de Gennes, *Scaling Concepts in Polymer Physics* (Cornell University Press, Ithaca, NY, 1971); J. Chem. Phys. **72**, 4756 (1980).

[13] J. W. Cahn and J. E. Hilliard, J. Chem. Phys. **28**, 258 (1958); J. W. Cahn, *ibid.* **42**, 93 (1965); H. E. Cook, Acta Metall. **18**, 297 (1970).
[14] L.-T. Yan and X.-M. Xie, Macromolecules **39**, 2388 (2006); J. Chem. Phys. **126**, 064908 (2007).
[15] H. Tanaka, J. Phys.: Condens. Matter **13**, 4637 (2001).
[16] S. Puri and K. Binder, Phys. Rev. E **49**, 5359 (1994).
[17] S. C. Glotzer, Annu. Rev. Comput. Phys. **2**, 1 (1995).
[18] I. M. Lifshitz and V. V. Slyozov, J. Phys. Chem. Solids **19**, 35 (1961).
[19] K. Kawasaki and T. Nagai, Physica A **121**, 175 (1983); T. Nagai and K. Kawasaki, *ibid.* **120**, 587 (1983).
[20] It should be noted that Ball and Essery's numerical results demonstrate that the parallel structures can also be observed in the phase separation system near a surface by choosing appropriate noise term. [see R. C. Bao and R. L. H. Essery, J. Phys.: Condens. Matter 2, 10303 (1990)] Our work, leading to lamellar structures through double quench process, is yet much easier to implement experimentally. So, our approach implicates more potential practical applications to develop regular morphology with unusual physical properties.